Graphene interlayer for current spreading enhancement by engineering of barrier height in GaN-based light-emitting diodes

Jung-Hong Min,[1] Myungwoo Son,[2] Si-Young Bae,[1] Jun-Yeob Lee,[1] Joosun Yun,[4] Min-Jae Maeng,[5] Dae-Gyeon Kwon,[5] Yongsup Park,[5] Jong-In Shim,[4] Moon-Ho Ham,[2, 3] and Dong-Seon Lee[1,*]

[1]*School of Information and Communications, Gwangju Institute of Science and Technology, Gwangju 500-712, South Korea*

[2]*Department of Nanobio Materials and Electronics, Gwangju Institute of Science and Technology, Gwangju 500-712, South Korea*

[3]*School of Materials Science and Engineering, Gwangju Institute of Science and Technology, Gwangju 500-712, South Korea*

[4]*Department of Electronic & Communication Engineering, Hanyang University, ERICA Campus, Ansan 426-791, South Korea*

[5]*Department of Physics and the Research Institute for Basic Sciences, Kyung Hee University, Seoul 130-701, South Korea*

[*]*dslee66@gist.ac.kr*

Abstract: Pristine graphene and a graphene interlayer inserted between indium tin oxide (ITO) and *p*-GaN have been analyzed and compared with ITO, which is a typical current spreading layer in lateral GaN LEDs. Beyond a certain current injection, the pristine graphene current spreading layer (CSL) malfunctioned due to Joule heat that originated from the high sheet resistance and low work function of the CSL. However, by combining the graphene and the ITO to improve the sheet resistance, it was found to be possible to solve the malfunctioning phenomenon. Moreover, the light output power of an LED with a graphene interlayer was stronger than that of an LED using ITO or graphene CSL. We were able to identify that the improvement originated from the enhanced current spreading by inspecting the contact and conducting the simulation.

OCIS codes: (230.0230) Optical devices; (160.6000) Semiconductor materials; (230.3670) Light-emitting diodes.

References and links

1. H. Zhao, G. Liu, J. Zhang, J. D. Poplawsky, V. Dierolf, and N. Tansu, "Approaches for high internal quantum efficiency green InGaN light-emitting diodes with large overlap quantum wells," Opt. Express **19**(S4), A991–A1007 (2011).
2. D. F. Feezell, J. S. Speck, S. P. DenBaars, and S. Nakamura, "Semipolar (20 $\bar{2}$ $\bar{1}$) InGaN/GaN light-emitting diodes high-efficiency solid-state lighting," J. Disp. Technol. **9**, 190–198 (2013).
3. G. Liu, J. Zhang, C. K. Tan, and N. Tansu, "Efficiency-droop suppression by using large-bandgap AlGaInN thin barrier layers in InGaN quantum-well light-emitting diodes," IEEE Photonics J. **5**(2), 2201011 (2013).
4. K. T. Delaney, P. Rinke, and C. G. Van de Walle, "Auger recombination rates in nitrides from first principles," Appl. Phys. Lett. **94**(19), 191109 (2009).
5. C. K. Tan, J. Zhang, X. H. Li, G. Liu, B. O. Tayo, and N. Tansu, "First principle electronic properties of dilute-as GaNAs alloy for visible light emitters," J. Disp. Technol. **9**(4), 272–279 (2013).
6. V. K. Malyutenko, S. S. Bolgov, and A. D. Podoltsev, "Current crowding effect on the ideality factor and efficiency droop in blue lateral InGaN/GaN light emitting diodes," Appl. Phys. Lett. **97**(25), 251110 (2010).
7. G. Jo, M. Choe, C. Y. Cho, J. H. Kim, W. Park, S. Lee, W. K. Hong, T. W. Kim, S. J. Park, B. H. Hong, Y. H. Kahng, and T. Lee, "Large-scale patterned multi-layer graphene films as transparent conducting electrodes for GaN light-emitting diodes," Nanotechnology **21**(17), 175201 (2010).
8. J. P. Shim, D. Kim, M. Choe, T. Lee, S. J. Park, and D. S. Lee, "A self-assembled Ag nanoparticle agglomeration process on graphene for enhanced light output in GaN-based LEDs," Nanotechnology **23**(25), 255201 (2012).
9. A. H. Castro Neto, F. Guinea, N. M. R. Peres, K. S. Novoselov, and A. K. Geim, "The electronic properties of graphene," Rev. Mod. Phys. **81**(1), 109–162 (2009).

#208118 - $15.00 USD Received 12 Mar 2014; revised 8 May 2014; accepted 10 May 2014; published 23 May 2014

10. X. Li, W. Cai, J. An, S. Kim, J. Nah, D. Yang, R. Piner, A. Velamakanni, I. Jung, E. Tutuc, S. K. Banerjee, L. Colombo, and R. S. Ruoff, "Large-area synthesis of high-quality and uniform graphene films on copper foils," Science **324**(5932), 1312–1314 (2009).
11. K. S. Kim, Y. Zhao, H. Jang, S. Y. Lee, J. M. Kim, K. S. Kim, J. H. Ahn, P. Kim, J. Y. Choi, and B. H. Hong, "Large-scale pattern growth of graphene films for stretchable transparent electrodes," Nature **457**(7230), 706–710 (2009).
12. G. Williams, B. Seger, and P. V. Kamat, "TiO2-graphene nanocomposites. UV-assisted photocatalytic reduction of graphene oxide," ACS Nano **2**(7), 1487–1491 (2008).
13. C. R. Dean, A. F. Young, I. Meric, C. Lee, L. Wang, S. Sorgenfrei, K. Watanabe, T. Taniguchi, P. Kim, K. L. Shepard, and J. Hone, "Boron nitride substrates for high-quality graphene electronics," Nat. Nanotechnol. **5**(10), 722–726 (2010).
14. S. Kim, D. H. Shin, C. O. Kim, S. S. Kang, J. M. Kim, C. W. Jang, S. S. Joo, J. S. Lee, J. H. Kim, S. H. Choi, and E. Hwang, "Graphene p-n vertical tunneling diodes," ACS Nano **7**(6), 5168–5174 (2013).
15. M. S. Choi, G. H. Lee, Y. J. Yu, D. Y. Lee, S. H. Lee, P. Kim, J. Hone, and W. J. Yoo, "Controlled charge trapping by molybdenum disulphide and graphene in ultrathin heterostructured memory devices," Nat. Commun. **4**, 1624 (2013).
16. S. K. Lee, H. Y. Jang, S. Jang, E. Choi, B. H. Hong, J. Lee, S. Park, and J. H. Ahn, "All graphene-based thin film transistors on flexible plastic substrates," Nano Lett. **12**(7), 3472–3476 (2012).
17. B. J. Kim, H. Jang, S. K. Lee, B. H. Hong, J. H. Ahn, and J. H. Cho, "High-performance flexible graphene field effect transistors with ion gel gate dielectrics," Nano Lett. **10**(9), 3464–3466 (2010).
18. T. H. Han, Y. Lee, M. R. Choi, S. H. Woo, S. H. Bae, B. H. Hong, J. H. Ahn, and T. W. Lee, "Extremely efficient flexible organic light-emitting diodes with modified graphene anode," Nat. Photonics **6**(2), 105–110 (2012).
19. N. Han, T. V. Cuong, M. Han, B. D. Ryu, S. Chandramohan, J. B. Park, J. H. Kang, Y. J. Park, K. B. Ko, H. Y. Kim, H. K. Kim, J. H. Ryu, Y. S. Katharria, C. J. Choi, and C. H. Hong, "Improved heat dissipation in gallium nitride light-emitting diodes with embedded graphene oxide pattern," Nat. Commun. **4**, 1452 (2013).
20. K. Chung, C. H. Lee, and G. C. Yi, "Transferable GaN layers grown on ZnO-coated graphene layers for optoelectronic devices," Science **330**(6004), 655–657 (2010).
21. X. Miao, S. Tongay, M. K. Petterson, K. Berke, A. G. Rinzler, B. R. Appleton, and A. F. Hebard, "High efficiency graphene solar cells by chemical doping," Nano Lett. **12**(6), 2745–2750 (2012).
22. S. Thongrattanasiri, F. H. L. Koppens, and F. J. García de Abajo, "Complete optical absorption in periodically patterned graphene," Phys. Rev. Lett. **108**(4), 047401 (2012).
23. B. J. Kim, C. Lee, Y. Jung, K. H. Baik, M. A. Mastro, J. K. Hite, C. R. Eddy, Jr., and J. Kim, "Large-area transparent conductive few-layer graphene electrode in GaN-based ultra-violet light-emitting diodes," Appl. Phys. Lett. **99**(14), 143101 (2011).
24. B. J. Kim, C. Lee, M. A. Mastro, J. K. Hite, C. R. Eddy, Jr., F. Ren, S. J. Pearton, and J. Kim, "Buried graphene electrodes on GaN-based ultra-violet light-emitting diodes," Appl. Phys. Lett. **101**(3), 031108 (2012).
25. X. Wang, L. Zhi, and K. Müllen, "Transparent, conductive graphene electrodes for dye-sensitized solar cells," Nano Lett. **8**(1), 323–327 (2008).
26. J. M. Lee, H. Y. Jeong, K. J. Choi, and W. I. Park, "Metal/graphene sheets as p-type transparent conducting electrodes in GaN light emitting diodes," Appl. Phys. Lett. **99**(4), 041115 (2011).
27. Z. Li, J. Kang, Z. Liu, C. Du, X. Lee, X. Li, L. Wang, X. Yi, H. Zhu, and G. Wang, "Enhanced performance of GaN-based light-emitting diodes with graphene/Ag nanowires hybrid films," AIP Adv. **3**(4), 042134 (2013).
28. X. Kun, X. Chen, D. Jun, Z. Yanxu, G. Weiling, M. Mingming, Z. Lei, and S. Jie, "Graphene transparent electrodes grown by rapid chemical vapor deposition with ultrathin indium tin oxide contact layers for GaN light emitting diodes," Appl. Phys. Lett. **102**(16), 162102 (2013).
29. J. P. Shim, T. H. Seo, J. H. Min, C. M. Kang, E. K. Suh, and D. S. Lee, "Thin Ni film on graphene current spreading layer for GaN-based blue and ultra-violet light-emitting diodes," Appl. Phys. Lett. **102**(15), 151115 (2013).
30. K. Joo, S. K. Jerng, Y. S. Kim, B. Kim, S. Moon, D. Moon, G. D. Lee, Y. K. Song, S. H. Chun, and E. Yoon, "Reduction of graphene damages during the fabrication of InGaN/GaN light emitting diodes with graphene electrodes," Nanotechnology **23**(42), 425302 (2012).
31. D. H. Youn, Y. J. Yu, H. Choi, S. H. Kim, S. Y. Choi, and C. G. Choi, "Graphene transparent electrode for enhanced optical power and thermal stability in GaN light-emitting diodes," Nanotechnology **24**(7), 075202 (2013).
32. Y. Wang, S. W. Tong, X. F. Xu, B. Özyilmaz, and K. P. Loh, "Interface engineering of layer-by-layer stacked graphene anodes for high-performance organic solar cells," Adv. Mater. **23**(13), 1514–1518 (2011).
33. X. Li, Y. Zhu, W. Cai, M. Borysiak, B. Han, D. Chen, R. D. Piner, L. Colombo, and R. S. Ruoff, "Transfer of large-area graphene films for high-performance transparent conductive electrodes," Nano Lett. **9**(12), 4359–4363 (2009).
34. H. J. Shin, W. M. Choi, D. Choi, G. H. Han, S. M. Yoon, H. K. Park, S. W. Kim, Y. W. Jin, S. Y. Lee, J. M. Kim, J. Y. Choi, and Y. H. Lee, "Control of electronic structure of graphene by various dopants and their effects on a nanogenerator," J. Am. Chem. Soc. **132**(44), 15603–15609 (2010).
35. X. Guo and E. F. Schubert, "Current crowding and optical saturation effects in GaInN/GaN light-emitting diodes grown on insulating substrates," Appl. Phys. Lett. **78**(21), 3337–3339 (2001).
36. Z. Ni, Y. Wang, T. Yu, and Z. Shen, "Raman spectroscopy and imaging of graphene," Nano Res. **1**(4), 273–291 (2008).

#208118 - $15.00 USD Received 12 Mar 2014; revised 8 May 2014; accepted 10 May 2014; published 23 May 2014

37. A. C. Ferrari, J. C. Meyer, V. Scardaci, C. Casiraghi, M. Lazzeri, F. Mauri, S. Piscanec, D. Jiang, K. S. Novoselov, S. Roth, and A. K. Geim, "Raman spectrum of graphene and graphene layers," Phys. Rev. Lett. **97**(18), 187401 (2006).
38. Y. Park, V. Choong, Y. Gao, B. R. Hsieh, and C. W. Tang, "Work function of indium tin oxide transparent conductor measured by photoelectron spectroscopy," Appl. Phys. Lett. **68**(19), 2699–2701 (1996).
39. T. H. Seo, K. J. Lee, A. H. Park, C. H. Hong, E. K. Suh, S. J. Chae, Y. H. Lee, T. V. Cuong, V. H. Pham, J. S. Chung, E. J. Kim, and S. R. Jeon, "Enhanced light output power of near UV light emitting diodes with graphene / indium tin oxide nanodot nodes for transparent and current spreading electrode," Opt. Express **19**(23), 23111–23117 (2011).
40. X. Kun, X. Chen, D. Jun, Z. Yanxu, G. Weiling, M. Mingming, Z. Lei, and S. Jie, "Graphene transparent electrodes grown by rapid chemical vapor deposition with ultrathin indium tin oxide contact layers for GaN light emitting diodes," Appl. Phys. Lett. **102**(16), 162102 (2013).
41. J. Yun, J. I. Shim, and D. S. Shin, "Current, voltage and temperature distribution modeling of light-emitting diodes based on electrical and thermal circuit analysis," Semicond. Sci. Technol. **28**(8), 085001 (2013).
42. J. Yun, D. P. Han, J. I. Shim, and D. S. Shin, "Three-dimensional analysis of temperature distributions based on circuit modeling of light-emitting diodes," IEEE Trans. Electron. Dev. **59**(6), 1799–1802 (2012).

1. Introduction

Lateral-type GaN-based light-emitting diodes (LEDs) have recently been immensely improved and commercialized for various applications, including general lighting. This has been possible in large part due to the use of current spreading layers (CSLs) in LEDs; these layers uniformly spread the current, thereby alleviating current crowding. While the significant factors obstructing the efficiency droop and internal quantum efficiency in vertical LEDs are based on charge separation [1, 2], carrier leakages [3], and Auger process [4, 5], the current crowding limits the efficiency-droop in lateral based LEDs [6]. Although thin metal layers or indium tin oxide (ITO) have been used as CSLs in GaN-based LEDs, drawbacks, such as severely degraded transmittance in the thin metal layers and steady price increases of indium, have prompted searches for alternative materials [7, 8]. Graphene, spotlighted as one such material, is a two-dimensional sheet composed of carbon held together by sp^2 hybridized bonds to form a hexagonal structure. This structure offers many advantages such as flexibility, high transparency, high conductivity, mechanical and chemical stability, and high thermal conductivity [9–13]. Due to these advantages, a variety of graphene applications and theories have recently been tested in electronic devices [14–17], optoelectronic devices [18–21], and optics [22]. Thus, graphene has recently started to take center stage in GaN-based LEDs as transparent electrodes, alternatively known as CSLs [7, 8, 23–33].

Without a CSL, a phenomenon called current crowding occurs in which current flow converges at the metal pad in GaN-based LEDs. The problem disappears with the use of a CSL due to the lower sheet resistance and proper work function. In this respect, graphene sheets have advantages when used as CSLs; Jo et al. have reported the superiority of graphene CSLs in GaN-based LEDs [7]. However, high sheet resistance and low work function of pristine graphene compared with those characteristics of conventionally used CSL materials, such as thin metal layers and ITO, cause a high turn-on voltage with insufficient current spreading [28]. Kim et al. even reported the malfunction of GaN-based near-ultra-violet LEDs with pristine graphene CSLs derived from oxygen [23, 24]. Thus, many attempts have been made to overcome these problems and improve the sheet resistance and work function of pristine graphene; these attempts have used methods such as graphene lamination, doping, metal layers, or combinations of various methods [18, 21, 26–28, 32–34]. However, even though Lee et al. used graphene sheets with metal layers to enhance current spreading in GaN-based LEDs, transmittance, one of the vital factors in CSLs, was found to degrade as metal layers became thicker [26]. Furthermore, while Han et al. demonstrated immense improvements in graphene transparent electrodes in organic LEDs by combining lamination and doping with graphene, they were not able to confirm the reliability of the modified graphene in GaN-based LEDs because of the different fabrication processes; additional layers were needed to enhance hole injection even with modified graphene [18].

Instead of using graphene as a CSL directly, a graphene interlayer between ITO and *p*-type GaN (*p*-GaN) can be one approach to improve current spreading, for the following reasons: (i) pristine graphene produces more than 95% transmittance in the visible range, and

#208118 - $15.00 USD Received 12 Mar 2014; revised 8 May 2014; accepted 10 May 2014; published 23 May 2014

thus as an interlayer would cause no degradation in transparency; (ii) pristine graphene, due to its high mobility, contributes to carrier transport; and (iii) the two-dimensional structure of graphene makes no change in the total thickness of the layers.

Here, we demonstrate the use of pristine graphene as CSLs and a graphene interlayer by inserting such a layer between the ITO and the *p*-GaN layer in GaN-based LEDs. First, LEDs with pristine graphene CSLs were unstable, leading to malfunction; this was confirmed to be originated from local damage by Joule heating due to the high sheet resistance and low work function of the pristine graphene. It was possible to resolve this problem by inserting a graphene interlayer, resulting in reduced sheet resistance. Moreover, the LEDs with inserted graphene between the ITO and the *p*-GaN layer exhibited improved light output power. The improvement most probably resulted from the increased current spreading length (L_s) and could be calculated as reported by Guo and Schubert [35]. The improvement can be explained as resulting from the graphene interlayer, which has high transparency and conductivity and acts as a two dimensional potential barrier with an intentionally increased Schottky barrier height at the interface between the ITO and the *p*-GaN.

2. Experiment

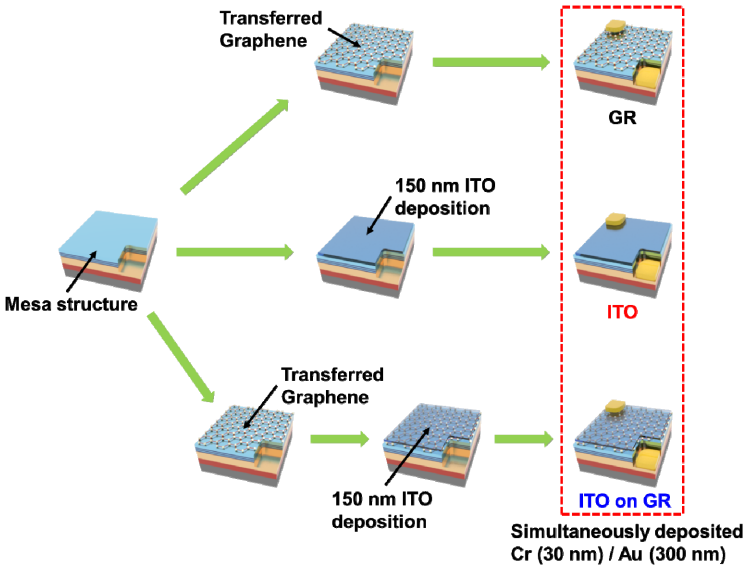

Fig. 1. Fabrication process of the three types of LEDs with different current spreading layers (CSLs). Based on a mesa structure, the LEDs were manufactured with a graphene current spreading layer ('GR'), 150-nm thick ITO CSL ('ITO'), and ITO on graphene interlayer ('ITO on GR').

Figure 1 schematically shows the fabrication of conventional lateral-type LEDs with different types of CSLs. We first grew blue LED structures having InGaN/GaN multi-quantum wells (MQWs) as an active layer using metal organic chemical vapor deposition (MOCVD). The full structures consisted of *p*-GaN/MQWs/*n*-GaN/un-doped GaN/sapphire substrate. To open the *p* and *n* regions, we deposited a 300 nm layer of SiO_2 on *p*-GaN as a mesa etching mask instead of using a conventional photoresist (PR), which gets severely denatured during inductive coupled plasma (ICP) etching [29, 30]. The mesa structures were patterned by photolithography on a 300-nm SiO_2 layer and were etched using reactive ion etching (RIE) to replicate the mesa pattern onto the SiO_2 layer. After ICP etching to expose *n*-GaN, the SiO_2 layer was removed by using a buffered oxide etchant for one hour, and mesa structures were completed.

On the base of these mesa structures, we fabricated three types of blue LEDs having different CSLs: pristine graphene only ('GR'), 150-nm thick ITO ('ITO'), and 150-nm thick

#208118 - $15.00 USD Received 12 Mar 2014; revised 8 May 2014; accepted 10 May 2014; published 23 May 2014

ITO with a graphene interlayer ('ITO on GR') [Fig. 1]. For the LED with 'GR', in order to transfer a sheet of graphene (Graphene Square, Seoul, Korea), a copper foil with graphene was attached to a polyethylene terephthalate (PET) film using a scotch tape to support the copper foil during spin coating. Polymethyl methacrylate (PMMA) was spin-coated at 3000 rpm for 1 min onto one side of the graphene layers grown on copper foil. The PET film supporting the copper foil with graphene coated by PMMA was separated from the copper foil with scissors. The copper foil with graphene-coated PMMA was then cured at 180 °C for 1 min. The graphene layer on the opposite side was removed by O_2-plasma treatment with RIE (O_2 50 sccm for 2 min 30 sec). The PMMA/graphene/copper foil layer was floated on $(NH_4)_2S_2O_8$ solution (0.098 g/mL) for 3 hours to etch away the copper foil. After repetitive rinsing with deionized water for cleaning, the PMMA/graphene layer was transferred onto the target substrate and dried slowly at room temperature for a day. Finally, the PMMA layer was removed using acetone at 80 °C for 1 hour, and the partial graphene was etched by O_2 plasma using RIE after ITO patterning using positive PR as a mask to make the graphene CSL. To remove the rest of the PR, the structure was dipped into acetone for 10 min; air-acetone spray was used with weak pressure for additional PR cleaning because numerous PR residues were generated during RIE. For the LED with 'ITO', the layer was deposited using e-beam evaporation on the mesa structures after PR patterning. The PR was then stripped and the ITO layer was subjected to rapid thermal annealing (RTA) at 600 °C in ambient air to crystallize it. For the LED with 'ITO on GR', the ITO layer was deposited using e-beam evaporation (150 nm thick ITO deposition with 1Å/s rate at room temperature) onto the ITO-patterned graphene sheet, already transferred onto the mesa-structured *p*-GaN by using previously mentioned transfer methods, and activated by RTA. Finally, we fabricated both the *p*- and *n*-type metal pads and deposited Cr/Au (30 nm/300 nm) as an ohmic contact.

3. Results and discussions

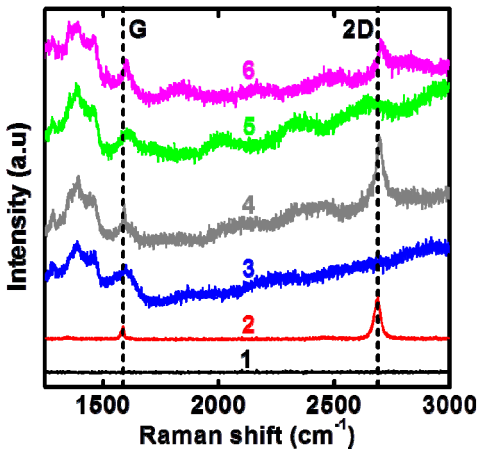

Fig. 2. Results of Raman spectroscopy. '1' through '6' show the Raman spectra with respect to sapphire, graphene transferred onto sapphire, GaN-based LED, graphene transferred on GaN-based LED, 'ITO' on GaN-based LED, and graphene interlayer between ITO and GaN-based LED, respectively. G and 2D peaks from graphene can be clearly observed in all graphene-containing samples.

After fabrication of the LEDs, we next verified the presence and type of graphene sheet through Raman spectroscopy (Ar laser, 514 nm) [Fig. 2]. A graphene sheet transferred to a double-polished sapphire layer (DPSL) clearly showed a G peak (1587 cm^{-1}) and a 2D peak (2688 cm^{-1}). The type of graphene used in this study was monolayer graphene because the intensity ratio of 2D to G was more than 2.5 and the full width half maximum of the 2D band was as small as 38 cm^{-1} [36, 37]. We also performed Raman spectroscopy on the three types of fabricated LEDs. Small shifts in the G and 2D peaks were observed, due mostly to defects

#208118 - $15.00 USD Received 12 Mar 2014; revised 8 May 2014; accepted 10 May 2014; published 23 May 2014

created during graphene transfer, scattering, and/or light absorption through ITO [36, 37]. The 'GR' and 'ITO on GR' LEDs showed the clear presence of transferred graphene, both exhibiting a G peak (1590 cm^{-1} (GR) and 1600 cm^{-1} (ITO on GR)) and a 2D peak (2700 cm^{-1} for both samples).

We prepared three different types of CSLs on the DPSL and also investigated the transmittance, sheet resistance, and work function. The CSLs best suited for lateral LEDs are required to have high transparency in the wavelength range of emissions, low sheet resistance for better current spreading, and proper work functions for better current injection.

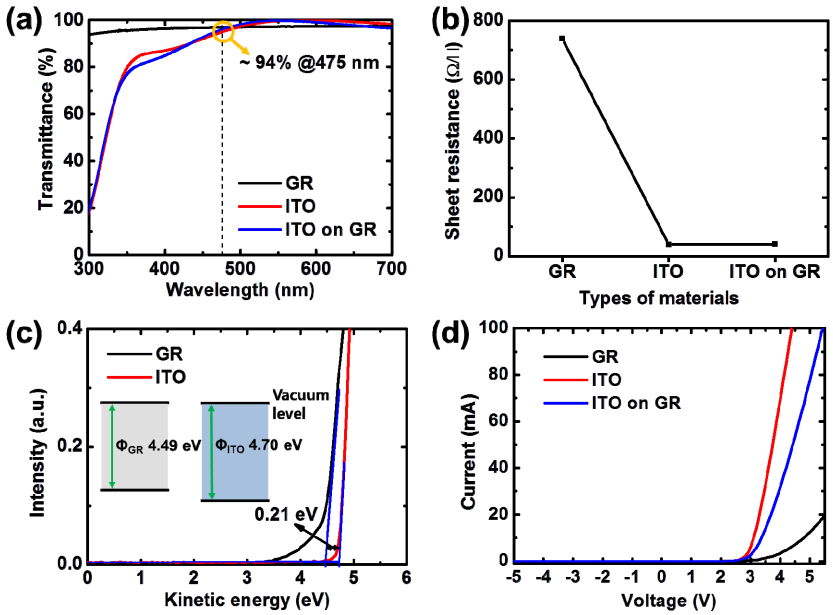

Fig. 3. (a) Transmittance values of 'GR', 'ITO', and 'ITO on GR'. (b) Sheet resistance of each material obtained by Hall measurements. (c) Work functions of 'GR' and 'ITO' measured by ultraviolet photoelectron spectroscopy [38]. (d) Current-voltage characteristics of 'GR', 'ITO', and 'ITO on GR'.

As can be seen in Fig. 3(a), the transmittances at 475 nm obtained using a UV/Vis/NIR absorption spectrophotometer were more than 94% for all three samples. In contrast, as can be seen in Fig. 3(b), the sheet resistance of 'GR' (739 Ω/□) was much higher than of either 'ITO' (~39 Ω/□) or 'ITO on GR' (~41 Ω/□), which were similar. Work functions were also measured for graphene and ITO using ultraviolet photoelectric spectroscopy. To form a good ohmic contact on the *p*-GaN, the work function of the material adhering to the *p*-GaN should be similar to or larger than that of *p*-GaN (i.e., larger than 6.5 eV). It is, however, hard to form an ideal ohmic contact on *p*-GaN using conventional materials because the largest work function of existing materials in the Periodic Table is that of selenium (5.9 eV), but this value is still smaller than that of *p*-GaN. From Fig. 3(c) and the insets, it can be seen that the work function of graphene (4.49 eV) is smaller than that of ITO (4.70 eV), which makes it more difficult for holes to flow from 'GR' or 'ITO on GR' CSL to *p*-GaN than it is for them to flow from 'ITO' to *p*-GaN. Based on the results of sheet resistances and work functions for each material in Fig. 3(d), we were able to determine that the I-V characteristic was poorest for 'GR' and best for 'ITO', which was just slightly better than that for 'ITO on GR'. From Fig. 3(d), the calculated series resistances of the CSLs can be seen to be 102.25 Ω, 13.67 Ω, and 21.79 Ω for GR, ITO, and ITO on GR, respectively.

Electroluminescence (EL) was studied in the three types of LEDs. The results for light output power and EL spectra are shown in Fig. 4.

#208118 - $15.00 USD Received 12 Mar 2014; revised 8 May 2014; accepted 10 May 2014; published 23 May 2014

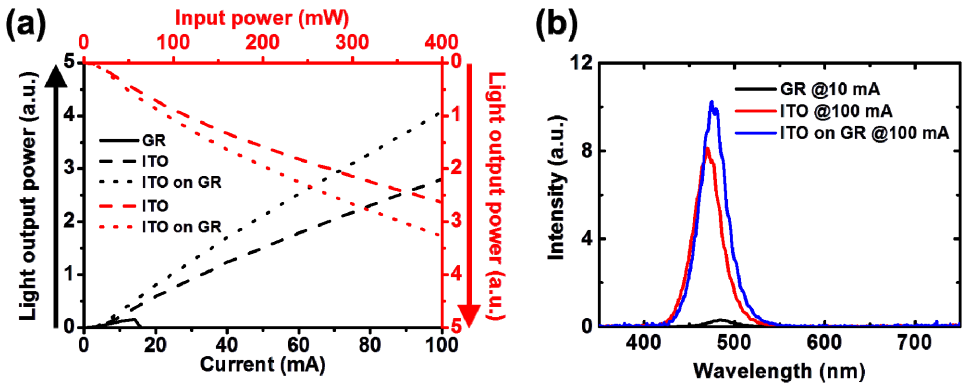

Fig. 4. (a) Light output power versus input current for 'GR', 'ITO', and 'ITO on GR' LEDs indicated by solid, dashed, and dotted black lines, respectively. Light output power versus input power for 'ITO' and 'ITO on GR' LEDs are also shown as dashed and dotted red lines, respectively. 'ITO on GR' showed a higher light output power than that of 'ITO'. (b) Electroluminescence spectra of 'ITO' and 'ITO on GR' LEDs at 100 mA; the spectra were taken at 10 mA for the 'GR' LED because of a malfunction of the LED at low current injection.

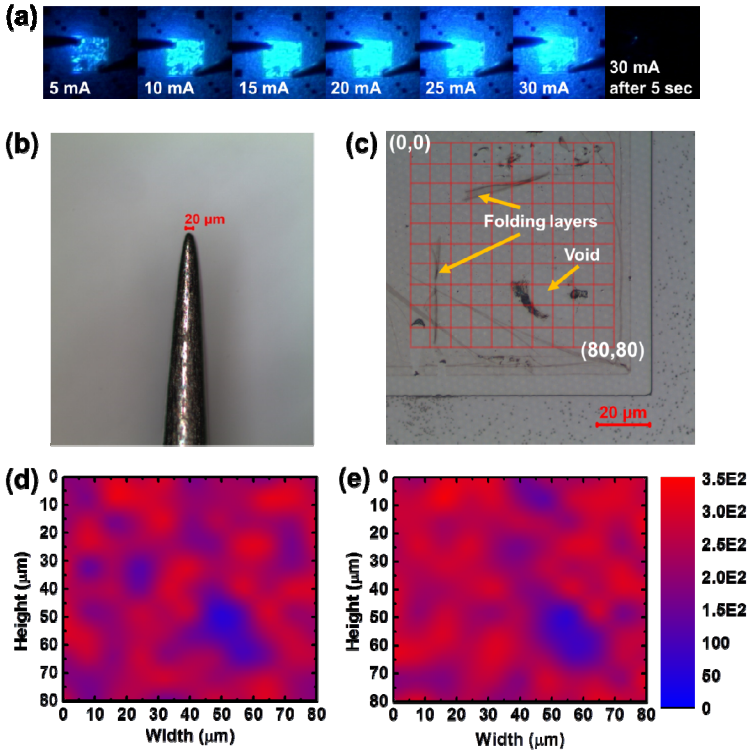

Fig. 5. (a) The electroluminescence (EL) image of the 'GR'. (b) An optical micro scope image of a probe-tip used in EL measurement. (c) An optical microscope image of the p-type metal pad region of the malfunctioning LED after removing the metal layers. Red-colored mesh represents the point of Raman mapping. Folding layers and a void are clearly observed. (d) and (e) show the results of Raman mapping using the intensity of G (1594 cm^{-1}) and 2D (2700 cm^{-1}), respectively.

#208118 - $15.00 USD Received 12 Mar 2014; revised 8 May 2014; accepted 10 May 2014; published 23 May 2014

Remarkably, the EL intensity for 'ITO on GR' was much stronger than that for 'ITO', although the electrical property of 'ITO' was better than that of 'ITO on GR'. Also, there was a curious phenomenon in the LEDs that used graphene CSL. From Fig. 4(a), it can be seen that the LED using graphene CSL became very unstable and eventually died when the injected current exceeded ~15 mA. Hence, the spectrum of the LED with GR had to be measured at 10 mA [Fig. 4(b)]. Kim et al. previously reported a similar malfunction in ultraviolet (UV) LEDs by oxygen contamination when using a single graphene sheet as a CSL [23]; this malfunction can be avoided by protecting the graphene CSL from oxygen using a SiO_2 layer [24].

We observed that the LED using a GR CSL gradually became dark as the injected current level was increased [Fig. 5(a)]. Having confirmed the presence of graphene in the GR CSL before current injection, we thought that the dying off of the LED must have originated from locally damaged graphene caused by the current concentrated at the *p*-type metal pad through the probe tip [Fig. 5(b)]. To verify this idea, we removed the *p*-type metal pad of the LED and directly investigated the graphene of the GR CSL; the graphene was found to have been damaged by the 30 mA current injection. It was possible to remove the *p*-type metal pads selectively, one at a time, using aqua regia for 30 s and Cr etchants for 10 s. The graphene was unharmed during the etching process because it has strong acid resistance. As can be seen in Fig. 5(c), the graphene beneath the *p*-type metal pad was uncovered to reveal a void almost as large as the probe tip on the graphene; some folded layers formed in transferring the graphene were also found. To confirm the presence of graphene in more detail, a Raman map was completed by setting a mesh over the p-type metal pad region with origin and end point indicated as (0, 0) and (80, 80), respectively [Fig. 5(c)]. The mapping results were determined with reference to the G peak (1594 cm^{-1}) and the 2D peak (2700 cm^{-1}) [Figs. 5(d) and 5(e)]. A huge void in the map was clearly observed at the same location as in the optical microscope image [Fig. 5(c)]. Thus, the current was clogged horizontally due to graphene's high sheet resistance; at the same time, the current was blocked vertically by the barrier formed from the difference in work functions between graphene and *p*-GaN, as shown in Fig. 6(b). These factors resulted in local damage to the graphene due to Joule heating as the injection current increased. Therefore, using monolayer graphene alone as a CSL proved unsuitable.

Thus, graphene's sheet resistance needs to be lowered if the material is to be used as a CSL. Stacking graphene into layers or depositing various types of thin metal layers (or metallic nanoparticles) onto the graphene is possible to reduce sheet resistance, although transmittance is degraded, resulting in a reduced extraction of light [7, 26, 27, 32–34]. However, by combining the graphene sheet as an interlayer with a 150-nm ITO layer, we not only solve the current crowding problem by improving the sheet resistance without degrading the transmittance, but also enhance the light output power. As we mentioned earlier, three conditions –high transmittance, low sheet resistance, and proper work function– determine whether or not some materials are suitable for use as CSLs. From that point of view, 'ITO' and 'ITO on GR' are much better than 'GR'. Seo et al. and Kun et al. previously reported that they inserted ITO dot/thin ITO layer between graphene and *p*-GaN, which means that ITO has been used for the contact material to enhance optical properties and current spreading [39, 40]. However, the light output power of the 'ITO on GR' LED was enhanced 45% compared with that of the 'ITO' LED for the same level of current injection (100 mA) in our result. The light output was also improved by 24.5% at the same power injection (400 mW).

#208118 - $15.00 USD Received 12 Mar 2014; revised 8 May 2014; accepted 10 May 2014; published 23 May 2014

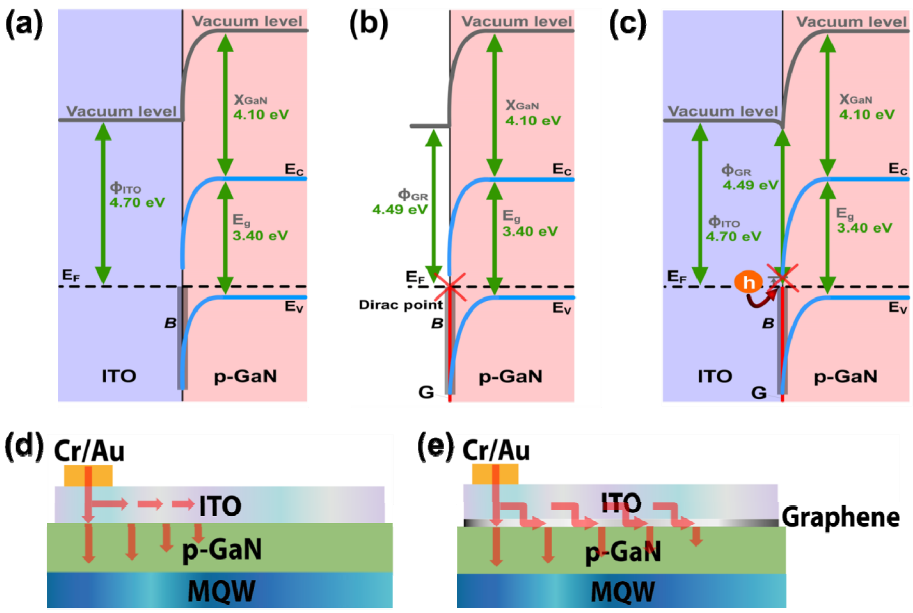

Fig. 6. (a), (b), and (c) show the band diagram of the CSLs and the *p*-type GaN: (a) ITO/*p*-type GaN, (b) graphene/*p*-type GaN, (c) ITO/graphene/p-type GaN. (d) and (e) show a schematic of the current flow from the p-type metal pad to the active layer through 'ITO' or 'ITO on GR' CSLs, respectively.

The enhancement in the light output power can be clearly explained by the improved current spreading. Previously, theoretical calculations reported by Guo and Schubert for current spreading length (L_s) resulted in the following equation [35]:

$$L_s = \sqrt{\frac{(\rho_c + \rho_p t_p) t_n}{\rho_n}} \tag{1}$$

where ρ_c is the specific *p*-type contact resistance, and $\rho_{p,\,n}$ and $t_{p,\,n}$ are the resistivity and thickness of the *p*- and *n*-type layers, respectively. According to Eq. (1), current spreading can be enhanced by increasing the specific contact resistance in the same LED structure. Although this seems contradictory because higher contact resistance usually deteriorates the electrical properties of LEDs, this increase of the specific contact resistance can actually contribute to the current spreading. Figures 6(a) and 6(c) show the energy band diagrams of 'ITO' and 'ITO on GR', respectively, at equilibrium state. According to the energy diagram, the Schottky barrier height (B), represented as thick grey lines, can be calculated according to:

$$B = E_g - (\phi_m - \chi_s) \tag{2}$$

where E_g is the bandgap of GaN, and ϕ_m and χ_s are the work function of the metallic materials and the electron affinity of GaN, respectively. The calculated heights with respect to 'ITO' and 'ITO on GR' are 2.8 eV and 3.01 eV, respectively. Based on the results of Eq. (2), In the case of 'ITO on GR', the barrier height, which is increased due to the inserting of the graphene interlayer, leads to a higher specific contact resistance and results in improved current spreading. By intuition, we can surmise that the elevated Schottky barrier blocks a portion of the current flow in the vertical direction; this blocked current can then take part in spreading horizontally for a short period of time, before eventually flowing vertically to the p-GaN. In that point of view, the current in the case of 'ITO on GR' flows better in the horizontal direction than does that of 'ITO', as shown in Figs. 6(d) and 6(e). Also, in order to explain the results in an experimental way, we evaluated the contact resistance values of

#208118 - $15.00 USD Received 12 Mar 2014; revised 8 May 2014; accepted 10 May 2014; published 23 May 2014

'ITO' and 'ITO on GR' using rectangular TLM: as had been supposed, the specific contact resistance of 'ITO on GR' was 0.31 Ω·cm^2, which is slightly higher than that of 'ITO', 0.22 Ω·cm^2. Thus, with the use of the graphene interlayer, the increased contact resistance consequently improves the current spreading without severe degradation in electrical properties.

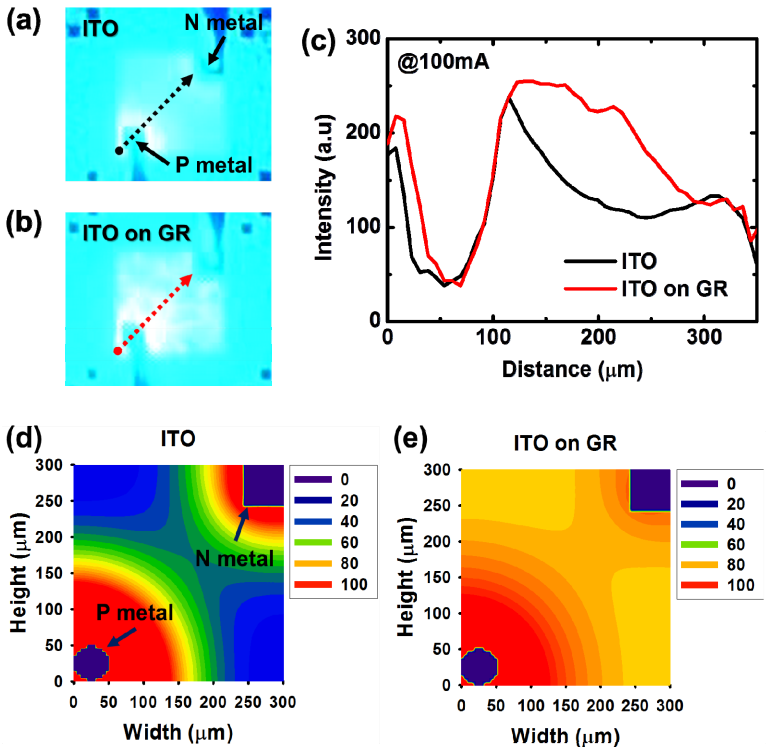

Fig. 7. (a) and (b) are optical microscope images of luminescence for 'ITO' and 'ITO on GR' LEDs at 100 mA. (c) Luminous intensity between the p-type and n-type metal pads, marked by black and red arrows in (a) and (b). Distance at x-axis signifies the length from the p-type metal pad to n-type metal pad. (d) and (e) are simulation results for current injection into the active layer through the 'ITO' or 'ITO on GR' CSLs.

Figures 7(a) and 7(b) provide microscope images of the light emission from the LEDs using the 'ITO' and 'ITO on GR' CSLs, respectively. To confirm the uniformity of the current distribution, we measured the light intensity using Matlab's image processing software over the area between the two metal pads, indicated as black- and red-colored dotted arrows in Figs. 7(a) and 7(b). Light intensity over distance values are plotted in Fig. 7(c). The region with very low intensity from ~20 μm to ~100 μm corresponds to the opaque p-type metal pad. The light intensity from the LED with an ITO CSL decreases significantly away from the p-type metal pad. In contrast, the light intensity from the LED with an 'ITO on GR' CSL was much more uniform, without any significant loss over the distance from the p-type metal pad to the n-type metal pad. Also, we simulated the current distribution through the active layer for both 'ITO' and 'ITO on GR' using chip design and analysis software (Design Optimizer for Scientific Applications simulation tool) [41, 42]. To perform this simulation, we designed all layers to be the same as they would be for real devices. The structure in the simulation was p-type metal pad/ITO/*p*-GaN/MQWs/*n*-GaN/n-type metal pad for 'ITO' and p-type metal pad/ITO/graphene/*p*-GaN/MQWs/*n*-GaN/n-type metal pad for 'ITO on GR'. In order to acquire the accurate simulation result, we exploit previously measured values, 39 Ω/□ and 41 Ω/□ for the sheet resistances and 2840 Ω and 14240 Ω for the contact resistance

#208118 - $15.00 USD Received 12 Mar 2014; revised 8 May 2014; accepted 10 May 2014; published 23 May 2014

of ‘ITO’ and ‘ITO on GR’, respectively. As can be seen in Figs. 7(d) and 7(e), the simulation results agreed well with the experimental ones in that the distribution of current for the ‘ITO on GR’ was more uniform, whereas a slight current crowding appeared at the edge of the p-type metal pad for the ‘ITO’ CSL.

4. Conclusion

In conclusion, we fabricated three types of GaN-based lateral LEDs using CSLs of ‘GR’, ‘ITO’, and ‘ITO on GR’. The ‘GR’ LEDs malfunctioned, forming a localized region of damage due to Joule heat arising from concentrated current, which was due mostly to high sheet resistance. The light output power of the ‘ITO on GR’ LED was the strongest of all samples, though this material had a slightly higher sheet resistance and smaller work function than those characteristics of the ‘ITO’ LED. The light output power of the ‘ITO on GR’ LED was enhanced by 45% compared with that of the ‘ITO’ LED at the same current condition and by 24.5% at the same input power of 400 mW. Based on the equation of current spreading length, the experimental results, and the simulation, we were able to confirm that, by inserting a graphene interlayer, the intentionally elevated Schottky barrier height leads to higher specific contact resistance in ‘ITO on GR’, and results in improved current spreading with no severe degradation of electrical or optical properties. Our results provide clear insight into the possibility using the insertion of a graphene sheet between the ITO and the *p*-GaN to improve current spreading via barrier height engineering.

Acknowledgments

This research was supported by Basic Science Research Program through the National Research Foundation of Korea (NRF) funded by the Ministry of Education, Science and Technology (No.NRF-2011-0015172) and the Core Technology Development Program for Next-generation Energy of Research Institute for Solar and Sustainable Energies (RISE), GIST.

#208118 - $15.00 USD Received 12 Mar 2014; revised 8 May 2014; accepted 10 May 2014; published 23 May 2014